

NASA/TM—2000-209769



# Cyclic Oxidation Testing and Modelling: A NASA Lewis Perspective

J.L. Smialek, J.A. Nesbitt, C.A. Barrett, and C.E. Lowell  
Glenn Research Center, Cleveland, Ohio

---

February 2000

## The NASA STI Program Office . . . in Profile

Since its founding, NASA has been dedicated to the advancement of aeronautics and space science. The NASA Scientific and Technical Information (STI) Program Office plays a key part in helping NASA maintain this important role.

The NASA STI Program Office is operated by Langley Research Center, the Lead Center for NASA's scientific and technical information. The NASA STI Program Office provides access to the NASA STI Database, the largest collection of aeronautical and space science STI in the world. The Program Office is also NASA's institutional mechanism for disseminating the results of its research and development activities. These results are published by NASA in the NASA STI Report Series, which includes the following report types:

- **TECHNICAL PUBLICATION.** Reports of completed research or a major significant phase of research that present the results of NASA programs and include extensive data or theoretical analysis. Includes compilations of significant scientific and technical data and information deemed to be of continuing reference value. NASA's counterpart of peer-reviewed formal professional papers but has less stringent limitations on manuscript length and extent of graphic presentations.
- **TECHNICAL MEMORANDUM.** Scientific and technical findings that are preliminary or of specialized interest, e.g., quick release reports, working papers, and bibliographies that contain minimal annotation. Does not contain extensive analysis.
- **CONTRACTOR REPORT.** Scientific and technical findings by NASA-sponsored contractors and grantees.

- **CONFERENCE PUBLICATION.** Collected papers from scientific and technical conferences, symposia, seminars, or other meetings sponsored or cosponsored by NASA.
- **SPECIAL PUBLICATION.** Scientific, technical, or historical information from NASA programs, projects, and missions, often concerned with subjects having substantial public interest.
- **TECHNICAL TRANSLATION.** English-language translations of foreign scientific and technical material pertinent to NASA's mission.

Specialized services that complement the STI Program Office's diverse offerings include creating custom thesauri, building customized data bases, organizing and publishing research results . . . even providing videos.

For more information about the NASA STI Program Office, see the following:

- Access the NASA STI Program Home Page at <http://www.sti.nasa.gov>
- E-mail your question via the Internet to [help@sti.nasa.gov](mailto:help@sti.nasa.gov)
- Fax your question to the NASA Access Help Desk at (301) 621-0134
- Telephone the NASA Access Help Desk at (301) 621-0390
- Write to:  
NASA Access Help Desk  
NASA Center for AeroSpace Information  
7121 Standard Drive  
Hanover, MD 21076

NASA/TM—1999-209769



# Cyclic Oxidation Testing and Modelling: A NASA Lewis Perspective

J.L. Smialek, J.A. Nesbitt, C.A. Barrett, and C.E. Lowell  
Glenn Research Center, Cleveland, Ohio

Prepared for the  
Cyclic Oxidation Workshop  
cosponsored by the Institute of Metals, European Federation of Corrosion, and DECHEMA  
Frankfurt, Germany, February 25–26, 1999

National Aeronautics and  
Space Administration

Glenn Research Center

---

February 2000

Trade names or manufacturers' names are used in this report for identification only. This usage does not constitute an official endorsement, either expressed or implied, by the National Aeronautics and Space Administration.

Available from

NASA Center for Aerospace Information  
7121 Standard Drive  
Hanover, MD 21076  
Price Code: A03

National Technical Information Service  
5285 Port Royal Road  
Springfield, VA 22100  
Price Code: A03

## **Cyclic Oxidation Testing and Modelling: A NASA Lewis Perspective**

James L. Smialek, James A. Nesbitt, Charles A. Barrett, and Carl E. Lowell  
National Aeronautics and Space Administration  
Glenn Research Center  
Cleveland, Ohio 44135

### **Abstract**

The Materials Division of the NASA Lewis Research Center has been heavily involved in the cyclic oxidation of high temperature materials for 30 years. Cyclic furnace and burner rig apparatus have been developed, refined, and replicated to provide a large scale facility capable of evaluating many materials by a standard technique. Material behavior is characterized by weight change data obtained throughout the test, which has been modelled in a step-wise process of scale growth and spallation. This model and a coupled diffusion model have successfully described cyclic behavior for a number of systems and have provided insights regarding life prediction and variations in the spalling process.

Performance ranking and mechanistic studies are discussed primarily for superalloys and coating alloys. Similar cyclic oxidation studies have been performed on steels, intermetallic compounds, thermal barrier coatings, ceramics, and ceramic composites. The most common oxidation test was performed in air at temperatures ranging from 800° to 1600°C, for times up to 10,000 h, and for cycle durations of 0.1 to 1000 h. Less controlled, but important, test parameters are the cooling temperature and humidity level. Heating and cooling rates are not likely to affect scale spallation. Broad experience has usually allowed for considerable focus and simplification of these test parameters, while still revealing the principal aspects of material behavior and performance. Extensive testing has been performed to statistically model the compositional effects of experimental alloys and to construct a comprehensive database of complex commercial alloys.

### **Background**

Many applications of high temperature materials require repeated heating and cooling cycles, thus demanding engineering materials that form slow growing oxides resistant to mechanical damage on cooldown. Large compressive stresses arise in scales during cooling because the thermal expansion coefficients of the substrate metals are generally 30-50% greater than those of the oxides. This in turn results in scale cracking, buckling, or delamination, and some degree of spallation, either within the scale thickness or at the scale-metal interface. The subsequent growth rate of the scale in the spalled region is higher because there is less oxide thickness through which the oxidant or metal must diffuse for continued reaction. The net result is that repeated cycling generally results in a greater material consumption rate. Consequently, cycle frequency, in addition to oxidation temperature, is an important degradation factor in applied oxidation cases.

Initial attempts at simulating the effects of cycling (ca. 1970) were accomplished by manual loading and unloading samples in an oxidation furnace, usually every 20 h, to obtain a daily sample weight and visual observation. However, the primary NASA Lewis interests in oxidation were turbine airfoil, combustor, or exhaust nozzle applications in aircraft engines. A more realistic cycle duration would be the 1-4 hour typical trip of a commercial aircraft. Consequently, manual furnace oxidation cycling evolved to once every 2 hours, but this required significant attention and was only practical for total test durations of 100 h or less.

### **Cyclic Furnace Testing**

Convenience and versatility dictated a more automated system, and the apparatus that evolved over the next ten years did away with the constant need of attention [1,2]. It employs a resistance furnace positioned vertically with six 3.5 cm diameter alumina tubes arranged in a hexagonal array. The specimen insertion device is a vertically oriented pneumatic cylinder above the furnace, which actuates a plate from which six platinum hangar wires and specimens are suspended. The piston travel and wire length are such that upon actuation the six specimens are lowered into the six tubes until reaching the center of the hot zone. Typical sample dimensions are 1-2 mm thick, 1-1.5 cm wide, and 2-3 cm long, resulting in nominally 2-5 gram samples for most first period transition metals. The NASA Lewis Cyclic Oxidation Facility contains ten FeCrAl Kanthal furnaces capable of 1200°C operation and four MoSi<sub>2</sub> Kanthal Super furnaces capable of 1600°C operation.

One tube contains a thermocouple, which continuously monitors the temperature at the specimen position. This has been found to agree well with a thermocouple spot welded to a sample. Thermal profiles revealed less than a 10°C variation over 10 cm of the hot zone. Heating rates were generally such that the test temperature was achieved in about 2 minutes. Cooling was accomplished by retraction of the hangar assembly as the specimens are pulled up into a chamber above the furnace to a final position about 10 cm above the furnace. A baffle plate is then automatically inserted between the samples and the chamber by another pneumatic mechanism. Cooling down to 50°C takes about 5 minutes for typical samples. All heating and cooling rates are exponential and unassisted by any flows other than natural convection. The heating and cooling cycle duration is electronically controlled by timers, and the number of cycles is controlled by a counter.

The following discussion highlights some of the important lessons learned over the years and incorporates the main findings of two cyclic oxidation spalling and diffusional loss computer models. Many of these points were initially raised in a review paper on cyclic oxidation [3]. This paper updates that review with new supporting data and raises some additional issues.

Cooling rate effects. While it appears intuitive and had been widely assumed that a higher cooling rate should induce greater thermal stress from a thermal shock component, in actuality it was found that a higher cooling rate actually decreased the weight loss rate and degree of spalling [3,4]. Rather than inducing a thermal gradient in thin scales, fast cooling by water quenching was found to induce large thermal gradients in the metal substrate. This resulted in the contraction of

the outer layer of substrate, opposed by the still-hot inner core. The surface is thus subjected to a shock-induced *tensile* component, and tensile deformation of the metal skin is actually observed. The scale is deformed along with the metal surface and may actually form cracks normal to the surface. This situation is much more resistant to spalling than intact scales subject to high compressive stresses. When the inner core of the metal is eventually cooled, its compressive effect on the scale is ameliorated by the intervening rigid, elongated skin of cool metal. The net effect is a significant reduction or reversal of the predicted compressive strain on the scale that would normally result from the higher thermal expansion of the substrate.

In the relevant experiment, samples of six superalloys either i) were manually removed from a vertical tube furnace at 1100°C and immersed in room temperature water or ii) remained hanging as the furnace was slowly lowered away from the specimens by a motorized drive mechanism [4]. The respective cooling times were about 5 seconds or 2400 seconds (40 min.), as compared to the usual 120-180 second (2-3 min.) air cooling in the conventional automated cyclic test. Weight change results are shown in Fig. 1. (Compositions for these and other alloys referred to later are listed in the original references or summary papers [28-31]). B-1900 and IN 601 showed considerably more severe degradation in **slow cooling** than in water quenching. IN 702 was somewhat worse, while Hoskins 875 and TD-Ni were unaffected by cooling rate. TD-NiCrAl was the only alloy tested that showed more weight loss in fast cool tests than in slow cool. But this was because the hard and brittle alloy cracked itself, rather than exhibit plastic surface deformation.

The significance of tensile straining the scale (from metal deformation by thermal shock) as opposed to compressive deformation (from the thermal expansion mismatch with the metal) was further illustrated by bending an oxidized 0.3 mm thick nickel strip to a 2.5 cm radius [4]. The strip had been oxidized at 1200°C for 100 hr. and slow cooled, but did not spall because of minimal thermal expansion mismatch. After bending, massive spallation was found for the compressive (concave) side, while an array of tensile cracks with no spalling was found on the tensile (convex) side. The cracks were similar to tensile cracks formed on the quenched IN 702 sample with improved behavior.

Cycle frequency effects. The vast majority of our tests have used a 1 hour heating and 20 minute cooling cycle. In special cases the cycle frequency may be increased, to provide a greater fatigue element, or decreased, to bias the test toward an isothermal exposure. It should be noted, however, that in some cases a relatively long cycle duration may provide the most severe material degradation. One explanation is that more frequent cycling may disrupt the scale by introducing a fine network of small cracks or spalled segments and so alleviate the massive strain energy built up by a single plate of oxide.

For example, in a study of undoped Ni-40Al, the most severe weight loss rates were experienced for 20-h cycle tests, followed by 50-h, then 1-h cycle tests, for the same amount of total time at temperature [5]. The measured amount of spalled area (to bare metal) was also greater for an isothermal test compared to the cyclic tests. However, in this particular case, the greater instance of interfacial void formation for long term exposures exaggerated the degree of spallation. Cycle frequency issues will be discussed further in the section on modelling.

Effect of cooling temperature. As discussed above, there is much data to indicate the overriding influence of thermal expansion mismatch in the generation of compressive stresses which lead to some degree of spallation. As a rule of thumb, the stress in the oxide will vary according to  $E_{ox}\Delta\alpha\Delta T$ . While  $E_{ox}$  and  $\Delta\alpha$  are both material parameters,  $\Delta T$  is fixed by the heating and cooling temperatures. The importance of the heating temperature is of course very well recognized, since it not only determines both the oxidation rate and thickness, but it also defines the upper limit to the span of the temperature change that induces the thermal stress. However, the cooling temperature is not always intentionally controlled. For example, the cooling chambers above our cyclic furnaces usually receive some degree of heating by convection. This will increase with furnace temperature, will vary with the ambient room temperature, and will also be subject to the seasonal trends in northeast Ohio.

To demonstrate whether the final cooling temperature is indeed important, Deadmore and Lowell varied  $\Delta T$  by controlling the final temperatures to which the samples were cooled, Fig. 2. [3,6].

For samples oxidized at 1100° or 1200°C for 195 h, but cooled only part way to room temperature, the amount of spallation was considerably reduced as one might expect. Furthermore, samples that were cycled below room temperature by immersion into liquid nitrogen (-196°C) incurred proportionally more severe spallation. For an 1100°C test of B-1900 and IN-601, an extra 0.75 mg cm<sup>-2</sup> was lost for every additional 100°C in cooling (i.e., about an extra 20% compared to the loss of about 4 mg cm<sup>-2</sup> for baseline cooling to room temperature). This effect was even greater for IN-718, even with an aluminide coating. For similar tests of IN 702 and TD-NiCrAlY at 1200°C, the increased weight loss was 1.5 mg cm<sup>-2</sup> for every additional 100°C in cooling (i.e., 50% worse compared to a baseline loss of about 3 mg cm<sup>-2</sup>). Only FeCrAl+Zr (Hoskins 875) was inert to this  $\Delta T$  effect, having never spalled because of excellent scale adherence, the extreme ductility of the alloy, and a better match in thermal expansion.

Implicit in these results is the prediction that measurable variations in weight loss will occur with naturally occurring random variations in the cooling temperature. This uncontrolled scatter may complicate very precise scientific investigations or preclude rigorous comparisons of cyclic data obtained from various laboratories. In most cases, however, this level of precision is not required, and overall alloy performance is reasonably duplicated by the simple test where cooling takes place above the furnace. While not the most elegant experimentally, the simplicity of this process has allowed for the comparisons of nearly a thousand alloys tested in the same laboratory under similar conditions for a number of temperatures [7].

Effect of humidity. In discussing random variations associated with the cooling temperature, ambient humidity effects must also be raised. A common observation among experimenters is that after initially cooling and weighing the sample, additional spallation may be both visually and gravimetrically observed by simply allowing the sample to sit away from the furnace area for a number of hours or days. This is related to the phenomenon referred to by the thermal barrier coating community as "cold spalling" "desktop spallation" or "the weekend effect."

In some cases this may be directly related to the decrease in interfacial bonding of alumina scales from exposure to moisture. We have made a number of observations on NiAl (1978) [5], NiCrAl (1986) [8], PWA 1480 (1989) [9], Rene'N5 (1994) [10], and PWA 1484 (1998) [11] stating that exposure to additional moisture after cooling resulted in a measurable increase in the amount of scale spallation, especially at the oxide-metal interface. These exposures may involve water immersion, suspension over a hot beaker of water, or simply breathing on the samples. A dramatic exhibition of this phenomenon occurred when Rene'N5 (+48 ppm wt. Y) was cycled for 500 1-h cycles at 1150°C and immersed in water. Oxidation produced a net weight gain (oxygen) of  $0.6 \text{ mg cm}^{-2}$ , i.e.,  $1.2 \text{ mg cm}^{-2}$  (oxide), or about  $3 \text{ }\mu\text{m}$  of scale. After immersion, an additional  $0.7 \text{ mg cm}^{-2}$  of oxide spalled, or about 60%. The amount of spalling to bare metal was visibly increased, Fig. 3. Similar tests have catalogued the amount of extra spallation due to moisture exposure over the duration of the test [10].

While water immersion is clearly an extreme, the fact that additional spallation occurs upon extended exposure to humid conditions means that random effects in the test results may arise. The frequency with which specimens are removed from the furnace location for weighing, the length of time that samples are left out, and the humidity in both the cooling chamber or the weighing area can all have an effect on the degree of spallation and performance in a cyclic test. Since these are not normally controlled, they pose an additional degree of uncertainty that will be difficult to eliminate for a large scale test program. For these, a common schedule for weight taking should be followed and the ambient humidity level should be noted.

### **Modelling Cyclic Oxidation and Life Prediction**

Spalling model. Generally cyclic oxidation weight change curves exhibit a basic shape consisting of an initial weight gain to a maximum value, a decrease followed by crossover to negative weight changes, and finally a nearly linear rate of weight loss. To further understand this in detail, the elements of cyclic oxidation have been computer modelled in a number of our studies [1, 5, 12, 13]. The process entails step-wise growing of a scale, spalling off a uniform portion of its thickness (or other specified spall distributions), and re-growth of the scale (at both spalled and intact regions). The intent of these efforts was to construct a reasonably faithful description of the process so that the functional dependencies of weight change curves on growth constant, cycle frequency, and spall constant could be shown. If agreement is obtained, the amount of metal consumed, very long-term behavior, or behavior for other cycle frequencies may all be calculated. It is not the purpose here to go into any detail on the development of the model, but rather to highlight the key findings and major implications on cyclic testing.

The model was referred to as COSP (Cyclic Oxidation Spalling Program), developed by Lowell et al., and described in a number of publications [1, 3, 12, 13, 14]. Another version called CYCLOX is available for PC use [13].

Some of the pertinent findings obtained from model studies are now described. If  $F$  is the fraction of oxide spalled per cycle, and  $W_r$  is the weight of the retained oxide just before cooling, then the spalling constant  $Q_o$  is defined as:

$$F = Q_o \cdot W_r^\alpha$$

where  $\alpha$  is an experimental constant, usually found to be approximately 1.0. (Alternatively, the weight of oxide spalled,  $W_s = Q_o W_r^2$ ). Then, for a parabolic growth constant of  $k_p$ , a stoichiometric constant of  $a$  (ratio of the weight of oxide to the weight of oxygen in the scale) and a cycle duration of  $\Delta t$ :

- the number of cycles to reach the maximum weight varies as:  $(k_p \Delta t Q_o^2)^{-1/3} a^{-2}$
- the time to cross zero weight,  $t_o$ , is  $\sim 3.3x$  the time to maximum weight,  $t_{max}$ .
- the maximum in the weight change curve  $(\Delta W/A)_{max}$  varies as:  $(k_p \Delta t / Q_o)^{1/3} a^{-3/4}$
- the final weight loss rate per hour,  $(dW/dt)_{final}$ , varies as:  $(k_p Q_o / \Delta t)^{1/3} a^2$

By simple inspection it can be seen that for a constant oxide phase (stoichiometric factor), increases in  $k_p$  or  $\Delta t$  will produce a systematic decrease in the number of cycles to reach maximum and zero weight change, as well as raise the level of the maximum weight change. An increase in the spall constant  $Q_o$  will also decrease the number of cycles to reach maximum and cross zero, decrease the level of the maximum weight gained, and increase the final loss rate.

The outputs of the model are the net weight change of the sample, the amount of scale present, the cumulative amount of oxide spalled, and the cumulative amount of metal consumed. An alternative procedure is to input actual oxidation data and determine the best fit to the experimental curve. This fit will define both a  $k_p$  and  $Q_o$  and allow re-calculation of the weight change curve, the oxide thickness, and the amount of metal consumed for any cycle frequency or total oxidation time. Thus, long-term implications may be obtained from less extensive cyclic tests.

To illustrate the parametric effects graphically, a number of cases were run by CYCLOX to generate families of curves where only one input parameter was varied. The results are shown in Fig. 4. Here some generic results for NiAl (+Zr) alloys have been modelled. In Fig. 4a, the effect of varying  $k_p$  of NiAl from 1000 to 1400°C is shown. Here a  $Q_o$  of about 0.0001 cm<sup>2</sup>·mg<sup>-1</sup> was chosen from previous model fits of actual 1200°C, 1-h cycle data (shown in Fig. 5). The compression of the curves to higher  $\Delta W/A_{max}$ , shorter  $t_{max}$  and  $t_o$ , and larger  $dW/dt_{final}$  weight loss slopes is apparent. In Fig. 4b, increases in cycle duration from 0.1 to 10 h show the steady increase in  $\Delta W/A_{max}$ ,  $t_{max}$  and  $t_o$  and the decrease in  $dW/dt_{final}$ . Finally, in Fig. 4c, for a 1200°C  $k_p$  and 1-h cycles, increases in the spall constant  $Q_o$  bring the curves from nearly isothermal behavior, through decreasing  $\Delta W/A_{max}$ ,  $t_{max}$  and  $t_o$ , to higher rates of  $dW/dt_{final}$ , ending with nearly immediate weight losses at  $Q_o = 0.1$  and 1.0.

Some comparisons with experimental curves are shown in the next few figures. First the model fit to an experimental curve is shown for Ni-48Al-0.1Zr (at.%) oxidized at 1200°C for 3000 h [14], Fig. 5. A  $k_p$  was assumed to be 0.02 mg<sup>2</sup>·cm<sup>-4</sup>·h<sup>-1</sup> from other work. Thus  $Q_o$  was then determined to be 0.000084 for this model fit. The agreement is very good.

Secondly, a well-behaved family of curves is shown in Fig. 6 for Ni-30Cr oxidized at 1050°C with varying cycle frequencies [1, 2]. Note that as the cycle duration is increased, the number of hours to cross zero is also increased. The predicted dependency should be as  $\Delta t^{2/3}$  for the number of *hours* to cross zero (i.e., as  $\Delta t^{-1/3}$  for the number of *cycles* to cross zero). A comparison of the predicted and actual dependence is shown in Fig. 7 for the data obtained for cycle durations of 10 min., 30 min., 1 h, and 5 h, where the predicted slope on a log-log plot should be 2/3.

While the basic shape of the cyclic oxidation curve can usually be fitted by this model and long term performance be approximated from a shorter term test, it is not always true that the performance measured with one cycle duration can be predicted from that measured with another. Another family of curves was obtained for MA 956 ( $Y_2O_3$  dispersed FeCrAlY) oxidized at 1200°C using 15 min., 1, 5, and 50 h cycles [15]. As shown in Fig. 8, the overall trend was to cross zero at longer times with a longer cycle duration, however, the 5 h  $\Delta t$  test actually crossed sooner than the 1-h  $\Delta t$  test.

Finally, some ostensibly peculiar behavior with cycle duration was observed for pure NiAl oxidized at 1100°C and Zr-doped NiAl oxidized at 1200°, 1250°, and 1300°C. Here only slight variations or even decreases in the number of hours to cross zero occurred with substantial increases in cycle duration (from 1 to 100 h), as shown in Fig. 9 [5, 14-16]. This phenomenon was discussed in relation to interface void formation and scale adhesion for undoped NiAl [5]. However for the Zr-doped NiAl, spalling occurred by transgranular cleavage within the scale and appeared similar for each cycle duration. Thus there was no apparent explanation of this behavior based on interface morphology.

In conclusion, it is important to point out that there is not necessarily a monotonic negative effect with increasing cycle frequency. Thus, each industrial need tends to evolve an approximate test standard with regard to cycle duration, such as 1-2 h cycles for aircraft turbines compared to thousands of hours for boiler applications. While some variations in cycle duration may be informative, extensive divergence from the intended use cycle may be misleading.

Mechanical aspects of the spalling model. This cyclic oxidation model was broadened to include effects arising from an increase in stress on the scale and normalized values of scale properties and fracture damage by Chan [16]. Trends in spalling behavior were derived as a function of  $\Delta T$ , the crack distribution in the scale, and the position of failure. Thus, different weight change behavior could be accounted for by different test or material parameters. Since NiAl scales exhibit variances in the normalized scale properties, it is not improbable that this is associated with the deviations from the expected cycle frequency effect.

Diffusion modelling and life prediction. If there are no mechanism changes, the total amount of oxidized element (i.e., Al or Cr) is eventually consumed, implying oxidation of a new, less protective component. In reality, this transition (or breakaway oxidation) will occur before total consumption. By modelling the diffusional behavior of the oxidized element in conjunction with its consumption by cyclic oxidation, the time to arrive at a critical Al or Cr content (i.e., failure or oxidative life) can be determined. The key parameters supplied by the cyclic model are the

amount of metal consumed,  $W_m$ , and its rate of consumption,  $dW_m/dt$ . Failure criteria may be based on total surface recession [18], depletion to a critical level of solute [19], or depletion to form a non-protective surface layer phase [20].

For the latter two criteria, the diffusion equation must be solved to predict concentration profiles. The rate of solute consumption  $dW_m/dt$  is used as a boundary condition at the oxide/metal interface and is equated to the solute flux in the alloy. During isothermal oxidation, the rate of metal consumption may be easily calculated from the parabolic rate constant. It is also inversely related to the oxide thickness. The time dependence of  $dW_m/dt$  can be used to yield a unique solution to the diffusion equation which, for a "semi-infinite" sample, incorporates a time independent solute concentration at the oxide/metal interface.

During cyclic oxidation, the oxide thickness does not increase in a monotonic fashion but decreases whenever spalling occurs on cooling. Thus, the rate of metal consumption discontinuously increases following each spalling event and is higher than that during isothermal oxidation. This higher rate of metal consumption also causes the solute concentration at the oxide/metal interface to decrease with time, resulting in shorter oxidative lifetimes, especially for "finite" thickness samples (coatings or thin sections) [21].

Because of the complex time dependence of this boundary condition, finite-difference diffusion models have been developed to predict concentration profiles for cyclic oxidation, coupled with the COSP spalling model. These models were used to predict the protective lifetime of an alumina-forming NiCrAlZr overlay coating on a simple Ni-Cr-Al [18] or Ni-base superalloy [22], as determined by a critical Al interface concentration. Fig. 10 shows an example of calculated and observed compositional profiles for a coated alloy after oxidation and diffusion at 1150°C for 100 h. The coating aluminum content has decreased from 25 to 6 at.% and diffused more than 200  $\mu\text{m}$  into the substrate.

Fig. 11 illustrates that the spalling model and spalling parameter,  $Q_o$ , can be used to predict the cyclic oxidation lifetime effect on coated substrates. Here a NiCrAl coating was modelled for 1200°C cyclic oxidation, assuming  $k_p \approx 0.01 \text{ mg}^2 \cdot \text{cm}^{-4} \cdot \text{h}^{-1}$ . For  $Q_o = 0.02$ , representing data obtained from a similar composition of bulk NiCrAl(Zr), lifetimes of about 1500 h are projected. For  $Q_o = 0.4$ , more representative of undoped MAI alloys, the lifetimes were only about 300 h. The model was also used to predict the oxidative lifetime in monolithic  $\beta$ -NiAl samples [19]. In this case, a decrease in Al content to approximately 38 at.%, resulted in the transformation from  $\beta$ -NiAl to less resistant  $\gamma'$ -Ni<sub>3</sub>Al and was therefore used as the failure criterion.

### **Comprehensive Data Sets (Compositional Effects and Performance Ranking)**

**Statistically designed test program.** A number of extensive cyclic oxidation studies involved statistical design of experiments. For example, a mapping study was used to define performance contours and to define an optimum composition in the Ni-Cr-Al system [23]. Also, partial factorial alloying designs were used to quantify elemental effects and develop an equation relating performance to composition for complex Ni-Co-Cr-Al-Ti-Ta-Nb-W-Mo superalloys

[24, 25]. In these and a number of other related studies, an approach was developed to combine the growth and spalling behavior into one figure of merit,  $k_a$ , called the attack parameter, where lower is better. This value was correlated with actual metal recession for a broad selection of alloys and was approximated as  $k_1 t^{1/2} + 10k_2 t$ , (where these parameters correspond to the growth and spalling constants in a "paralinear" curve fit to the cyclic oxidation weight change curve, i.e.,  $\Delta W/A = (k_1 t)^{1/2} - k_2 t$  [1, 23, 26]. Here  $k_1$  and  $k_2$  loosely correspond to  $k_p$  and  $(k_p Q_o)^{1/3}$ , which represent the growth constant and the final slope in the cyclic oxidation computer model.

Some generalizations drawn from these studies were summarized in other reviews of high temperature oxidation [27, 28]. In these it was illustrated that the cyclic behavior of both model and commercial superalloys is most improved by higher levels of aluminum and, to a lesser extent, tantalum. Chromium is only somewhat beneficial for the alloy sets studied, in part due to the fact that it is usually reduced when aluminum is increased in commercial alloys. Titanium most notably decreases oxidation resistance in both the model alloy data set and in the characterization of commercial alloys. The effect of cobalt content was not significant.

Idealized trends have been quantified as illustrated in Fig. 12. In this figure, an attack parameter was calculated from a multilinear regression equation developed from the 1100°C cyclic oxidation data of 34 commercial Ni-base superalloys [26]. A base alloy of Ni-8Cr-6Al-6Ta-4Mo-4W-1Nb (wt.%) was chosen as a simplified reference composition, having nearly the optimum  $k_a$  ( $\approx 0.1$ ) displayed by real alloys. The relative effects produced by varying one element at a time can be seen by comparing the individual elemental lines. Data points for some individual alloys (with different molybdenum, tungsten, niobium, hafnium, or vanadium contents) are also shown in comparison to the reference composition (dashed line).

There are a number of other related large-scale cyclic oxidation studies [29-31], some of which had been summarized and discussed in references 27 and 28. Much of the weight change data from all of these test programs is presently being consolidated in one single format by means of a CD-ROM [7] to allow for quick, convenient data retrieval and alloy comparisons.

## Summary

Various issues have been raised regarding the NASA Lewis experience with cyclic oxidation testing. It was shown that cooling rate does not necessarily increase the spallation amount. In fact, for a number of alloys, water quenching was seen to *reduce* spalling in comparison to slow furnace cooling because of thermal shock and tensile deformation of the underlying metal surface. The *amount* of cooling, however, typically led to higher compressive stresses and spallation, even when achieved by cooling below room temperature.

Increasing the cycle frequency is generally expected to increase the amount of spalling for a fixed total test duration. However, a number of exceptions have been noted. This emphasizes the need to simulate the intended application to avoid misleading conclusions. The frequency of removing the sample from the furnace area for weighing and inspection may also give rise to unexpected results. Spalling may be induced here because of further temperature reductions or exposure to

room moisture. This moisture effect was most noted for alumina scales that were only partially adherent because of an intermediate sulfur content or relatively low yttrium content.

The generic weight change behavior observed in cyclic oxidation tests was modelled by an iterative, step-wise computer calculation that employed the oxidation rate, the cycle duration, a spall constant, and the scale stoichiometry factor ( $k_p$ ,  $\Delta t$ ,  $Q_o$ , and  $a$ ). Systematic trends were observed in the model weight change curves as a function of these input parameters. Descriptive features ( $\Delta W/A_{max}$ ,  $t_{max}$ ,  $t_o$ , and  $dW/dt_{final}$ ), can be defined by mathematical functions of the input parameters. Actual weight change curves may be described nicely by a unique model fit (meaning  $k_p$  and  $Q_o$ ) for a given cycle duration and scale phase ( $\Delta t$  and  $a$ ). However, it appears that  $Q_o$  may sometimes display rather unexpected variations with oxidation temperature or cycle duration.

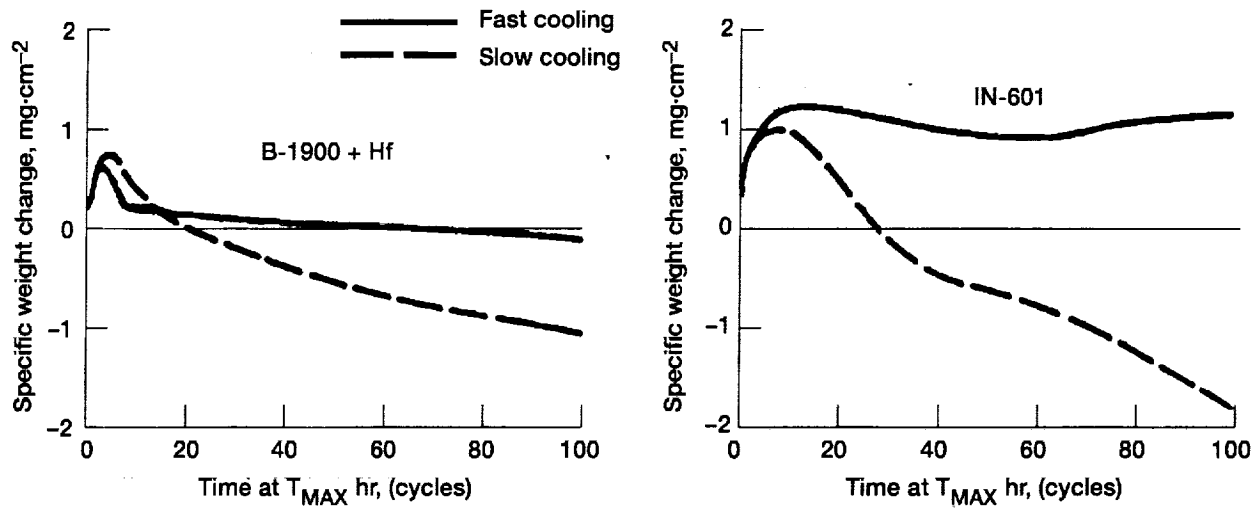
The cyclic model outputs were also coupled with a finite difference diffusion model to calculate diffusion profiles and solute loss in monolithic or coated articles. This allowed life prediction to be performed, assuming a critical solute content, depletion zone formation, or total material recession as criteria for oxidative failure.

Finally, large assemblies of cyclic data have been summarized through the use of a single attack parameter,  $k_a$ , that had been correlated with metal recession. This allowed for first level ranking of alloys by oxidative performance in a simple common test. This parameter was also modelled in terms of alloy composition for both statistically designed and commercially available alloys. Both approaches identified the primary benefits of aluminum content, followed by tantalum and chromium, over the range of compositions studied. The negative effects of titanium and vanadium were clear; molybdenum, tungsten, and niobium additions were less detrimental. No significant effect of cobalt content could be determined.

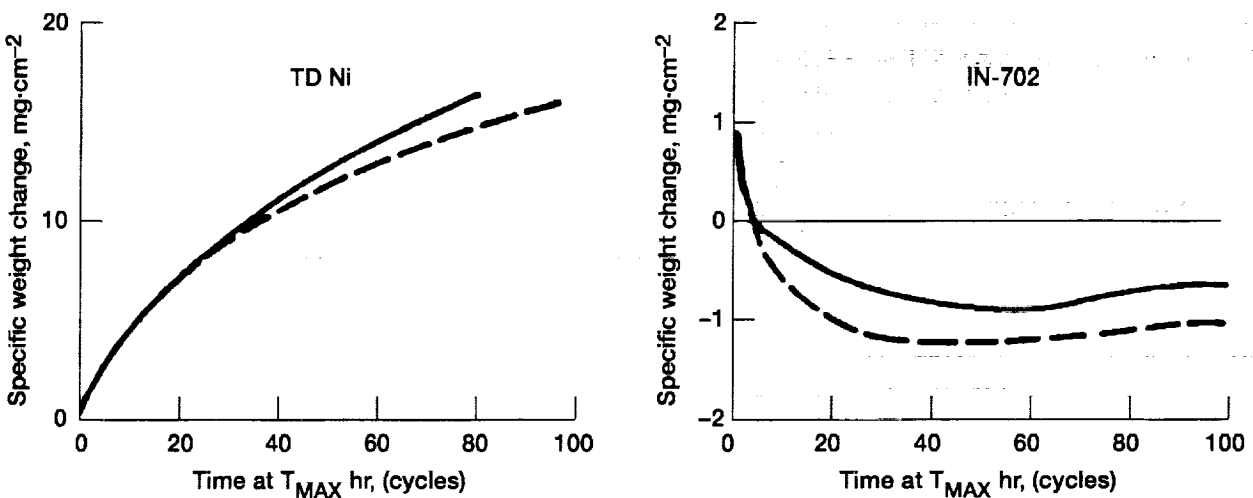
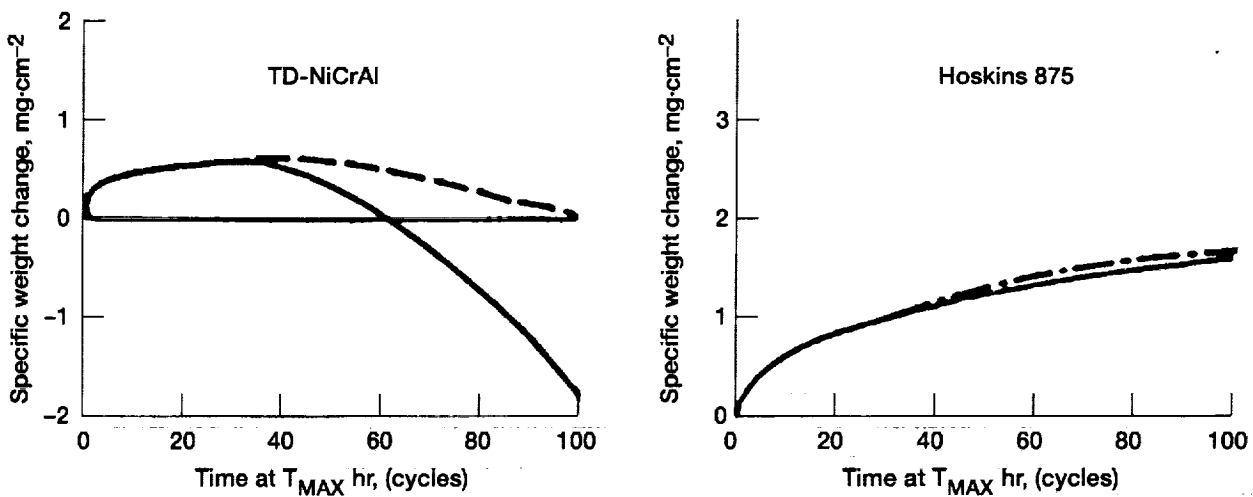
### References

1. C.A. Barrett and C.E. Lowell, "High Temperature Cyclic Oxidation Furnace Testing at NASA Lewis Research Center," *Journal of Testing and Evaluation*, JTEVA, 1982, Vol. 10, pp. 273-278, also NASA TM-81773, 1981.
2. C.E. Lowell, *Oxid. Met.*, 1973, 7, (2), 95-116.
3. C.E. Lowell, J.L. Smialek, and C.A. Barrett, "Cyclic Oxidation of Superalloys," in *High Temperature Corrosion*, NACE 6, (1981, San Diego, California), pp. 219-226, (R.A. Rapp, ed.), NACE, Houston, Texas, 1983.
4. C.E. Lowell and D.L. Deadmore, *Oxid. Met.*, 1980, 14, (4), 325-336.
5. J.L. Smialek, *Metall. Trans.*, 1978, 9A, 309-320.
6. D.L. Deadmore and C.E. Lowell, *Oxid. Met.*, 1977, 11, (2), 91-106.
7. C.A. Barrett, A CD-ROM Database of High Temperature Cyclic Furnace Oxidation of Alloys (unpublished research, 1999).
8. J.L. Smialek, "Adherent  $Al_2O_3$  Scales Produced on Undoped NiCrAl Alloys," in N.L. Peterson Memorial Symposium, *Oxidation of Metals and Associated Mass Transport*, (1986, Orlando, FL), pp.297-313, (M.A. Dayanada, S.J. Rothman, and W.E. King, eds.), TMS-AIME, Warrendale, Pennsylvania, 1987.

9. B.K. Tubbs and J.L. Smialek, "Effect of Sulfur Removal on Scale Adhesion to PWA 1480," in *Corrosion and Particle Erosion at High Temperatures*, (1989, Las Vegas, Nevada), pp. 459–486, (V. Srinivasan, K. Vedula, eds.), TMS-AIME, Warrendale, Pennsylvania, 1989.
10. J.L. Smialek, D.T. Jayne, J.C. Schaeffer, and W.H. Murphy, *Thin Solid Films*, 1994, 253, 285–292.
11. J.L. Smialek, unpublished research, 1998.
12. C.E. Lowell, C.A. Barrett, R.W. Palmer, J.V. Auping, and H.B. Probst, *Oxid. Met.*, 1991, 36, (1/2), 81–112.
13. H.B. Probst and C.E. Lowell, *J. Metals*, 1988, 40, 18–21.
14. C.A. Barrett, "The Effect of 0.1 Atomic Percent Zirconium on the Cyclic Oxidation Behavior of  $\beta$ -NiAl for 3000 h at 1200°C", in *Oxidation of High-Temperature Intermetallics*, (1988, Cleveland, Ohio), pp. 67–83, (T. Grobstein and J. Doychak, eds.), TMS-AIME, Warrendale, Pennsylvania.
15. C.A. Barrett and C.E. Lowell, unpublished research, 1998.
16. J.A. Nesbitt and C.A. Barrett, "Predicting the Oxidation-Limited Lifetime of  $\beta$ -NiAl," in *Structural Intermetallics*, (1993, Seven Springs Resort, Champion, PA), pp. 601–609, (R. Darolia et al., eds.), TMS-AIME, Warrendale, Pennsylvania, 1993.
17. K.S. Chan, *Metall. Mat. Trans.*, 1997, 28A, 411–422.
18. J.A. Nesbitt and C.E. Lowell, *Mat. Res. Soc. Symp. Proc.*, 1993, 288, 107–118.
19. J.A. Nesbitt and R.W. Heckel, *Thin Solid Films*, 1984, 119, 281–290.
20. J.A. Nesbitt and E.J. Vinarcik, "Predicting the Oxidative Lifetime of  $\beta$ -NiAl-Zr Alloys," in *Damage and Oxidation Protection*, 25-1, Book No. H0692A, pp. 9–22, (K. Haritos and O.O. Ochos, eds.), ASME, 1991.
21. J.A. Nesbitt, *J. Electrochem. Soc.*, 1989, 136, 1518–1527.
22. J.A. Nesbitt, "Diffusional Aspects of the High Temperature Oxidation of Protective Coatings," in *Diffusion Analysis and Applications*, pp. 307–324, (A.D. Romig and M.A. Dayanada, eds.), TMS-AIME, Warrendale, Pennsylvania, 1989.
23. C.A. Barrett and C.E. Lowell, *Oxid. Met.*, 1977, 11, (4), 199–223.
24. C.A. Barrett, R.V. Miner, and D.R. Hull, *Oxid. Met.*, 1983, 20, 255–278.
25. C.A. Barrett, NASA TM–83784, Washington, D.C., 1984.
26. C.A. Barrett, NASA TM–105934, Washington, DC, 1992.
27. J.L. Smialek and G.H. Meier, "High-Temperature Oxidation," in *Superalloys II*, Chapter 11, pp. 293–326, (C.T. Sims, N.S. Stoloff, and W.C. Hagel, eds.), Wiley, New York, New York, 1987.
28. J.L. Smialek, C.A. Barrett, and J.C. Schaeffer, "Design for Oxidation," in *ASM Handbook Vol.20, Materials Selection and Design*, pp. 589V602, ASM International, Materials Park, Ohio, 1997.
29. C.A. Barrett, "10,000 Hour Cyclic Oxidation Behavior at 815°C (1500°F) of 33 High-Temperature Alloys," in *Environmental Degradation of Materials*, pp. 319–327, Virginia Tech, Blacksburg, Virginia, 1977.
30. C.A. Barrett, "10,000 cyclic Oxidation Behavior at 982°C (1800°F) of 68 High-Temperature Co-, Fe-, and Ni-Base Alloys," NASA TM–107394, 1997.
31. C.A. Barrett, R.G. Garlick, and C.E. Lowell, "High-Temperature Cyclic Oxidation Data, Parts I and II," NASA TM–83665 and TM–101468, Washington, DC, 1989.

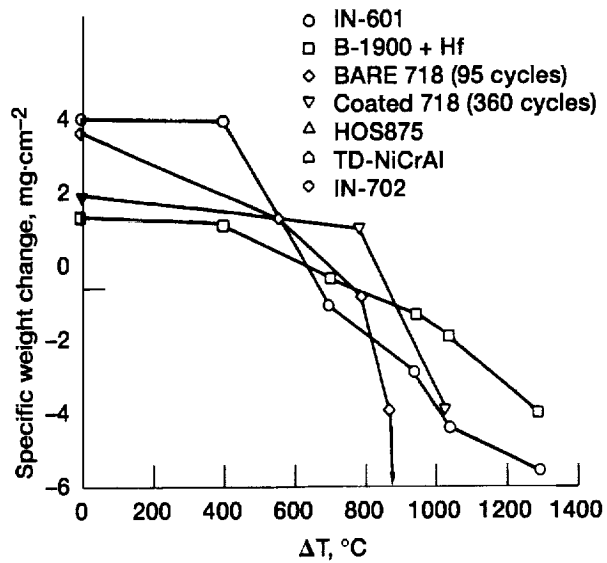


(a)  $T_{\text{MAX}} = 1100^\circ\text{C}$ ,  $\Delta T = 1050^\circ\text{C}$ .

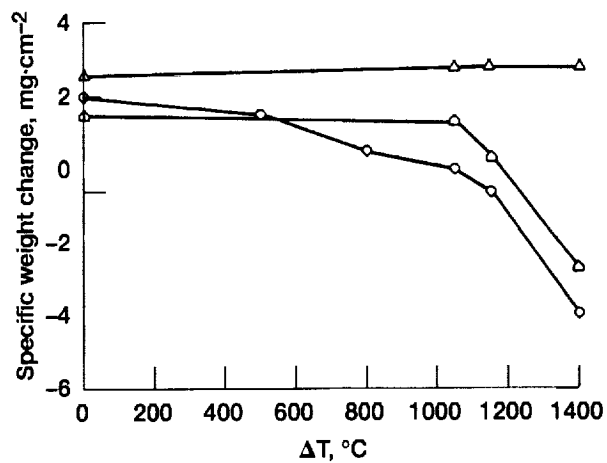


(b)  $T_{\text{MAX}} = 1200^\circ\text{C}$ ,  $\Delta T = 1150^\circ\text{C}$ .

Figure 1.—The effect of water quenching on the  $1100^\circ$  or  $1200^\circ\text{C}$ , 100-h cyclic oxidation behavior of six high temperature alloys. (Lowell and Deadmore, [4]).

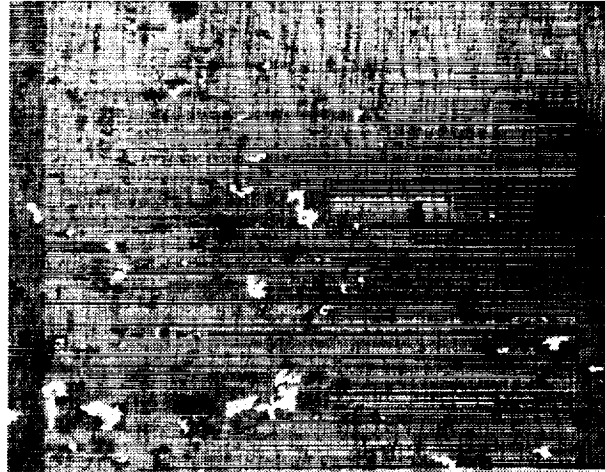


(a)  $T_{MAX} = 1100\text{ }^{\circ}\text{C}$

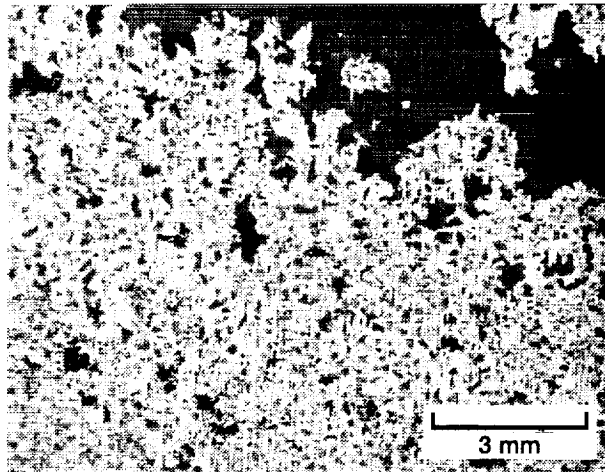


(b)  $T_{MAX} = 1200\text{ }^{\circ}\text{C}$

Figure 2.—The effect of  $T_{min}$  on the  $1100^{\circ}$  or  $1200\text{ }^{\circ}\text{C}$ , 200-h cyclic oxidation behavior of seven high temperature alloys.  $T_{min} = -196\text{ }^{\circ}\text{C}$  achieved by liquid nitrogen. (Deadmore and Lowell, [6]).



After cooling



After 1-h water immersion

Figure 3.—The effect of water immersion on the interfacial spalling for Rene N5 (48 ppmw Y) after oxidation for 500 1-h cycles at 1150 °C.

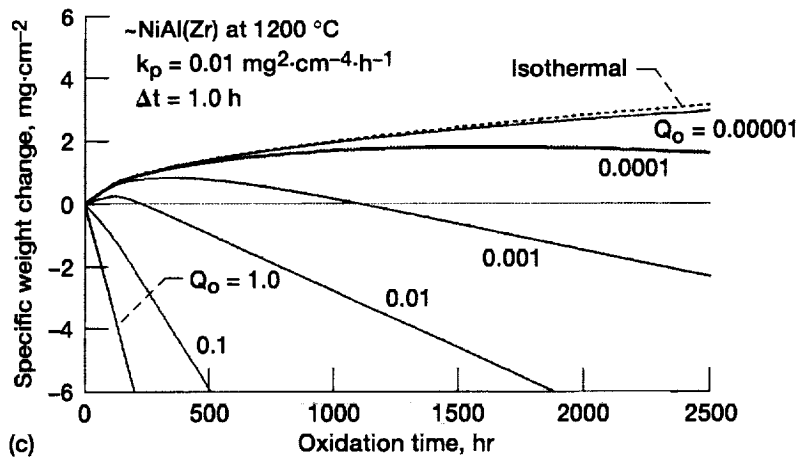
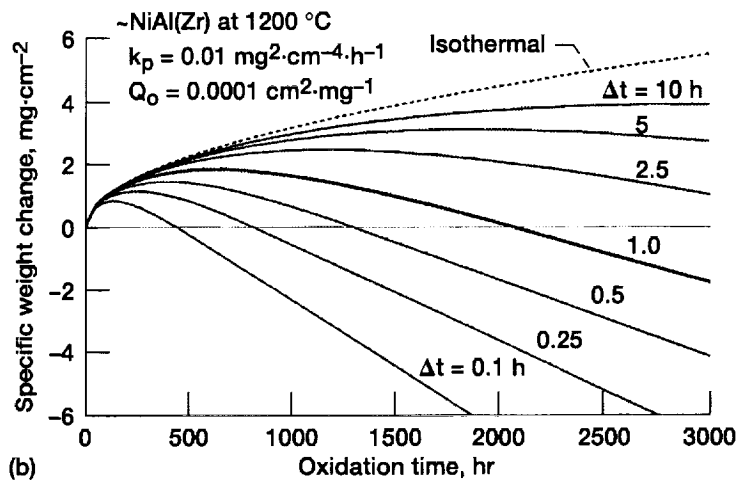
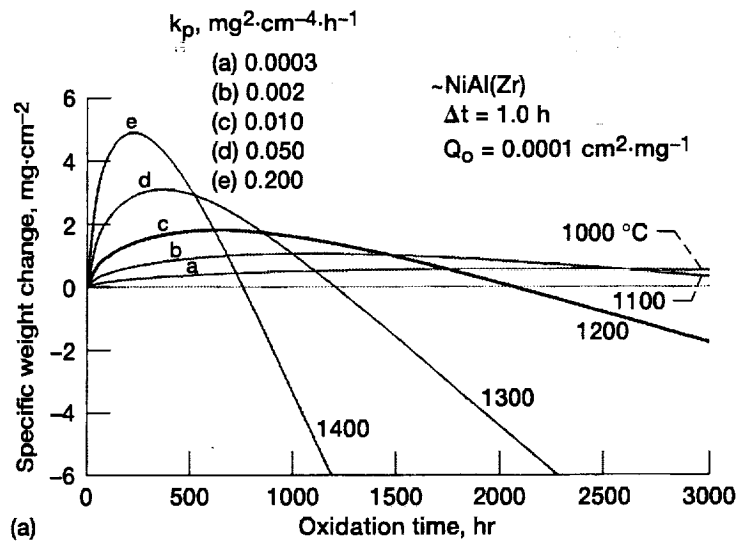


Figure 4.—The effect on families of model weight change curves generated by the CYCLOX cyclic oxidation model computer program. (a) Growth constant  $k_p$ . (b) Cycle duration  $\Delta t$ . (c) Spall constant  $Q_o$ .

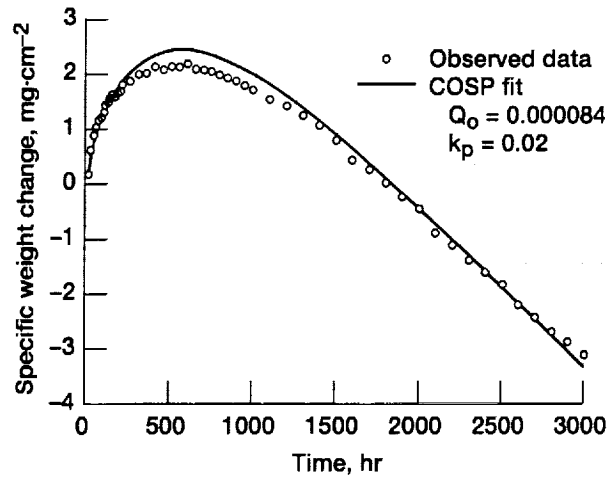


Figure 5.—Computer fit (COSP) agreement with actual data for Ni48Al-0.1Zr (at.%) oxidized at 1200 °C for 3000 1-h cycles.  $k_p = 0.02$ ,  $Q_0 = 0.000084$ . (Barrett, [14]).

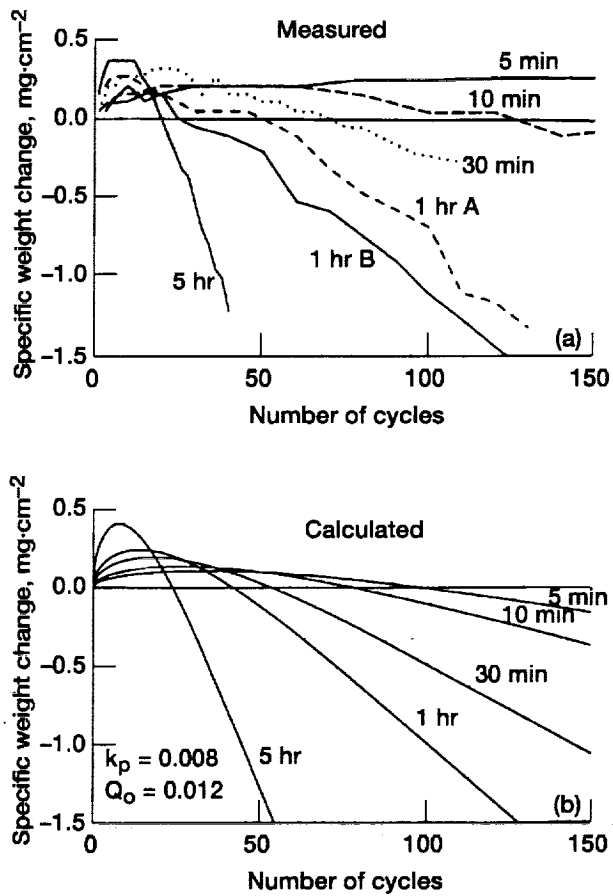


Figure 6.—The effect of cycle duration,  $\Delta t$ , on the cyclic weight change curves for Ni-30Cr oxidized at 1050 °C for 150-h.  $k_p = 0.008 \text{ mg}^2 \cdot \text{cm}^{-4} \cdot \text{h}^{-1}$ ,  $Q_0 = 0.012 \text{ cm}^2 \cdot \text{mg}^{-1}$  (Lowell et al., [12]).

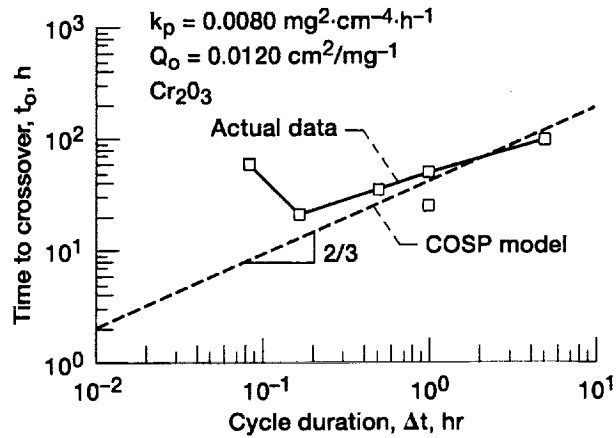


Figure 7.—Agreement of calculated and experimental effects of cycle duration,  $\Delta t$ , on the time to cross zero weight change for Ni-30Cr (from Fig. 5).

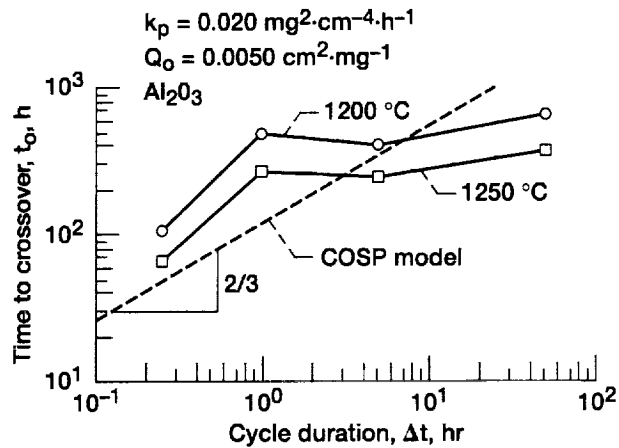


Figure 8.—The non-ideal effects of cycle duration,  $\Delta t$ , on the time to cross zero weight change for MA 956 oxidized at 1200 °C. (Lowell and Barrett, [15]).

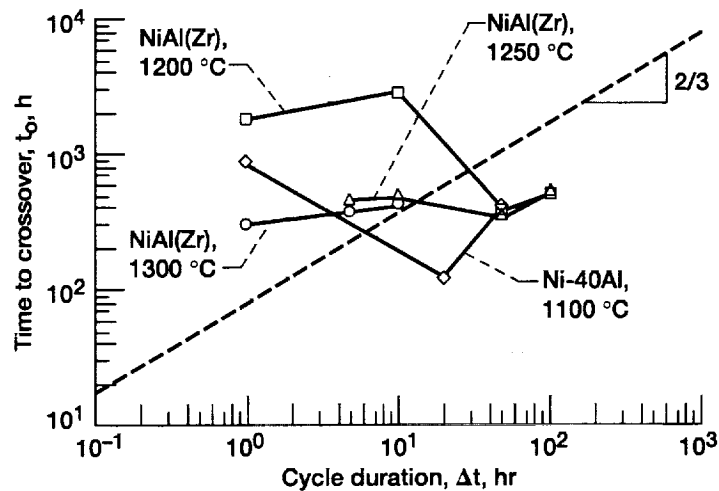


Figure 9.—The anomalous effects of cycle duration,  $\Delta t$ , on the time to cross zero weight change for NiAl ( $\pm$ Zr) oxidized at 1100-1300 °C. (Smialek, [5]; Nesbitt and Barrett, [16]; Lowell and Barrett, [15]).

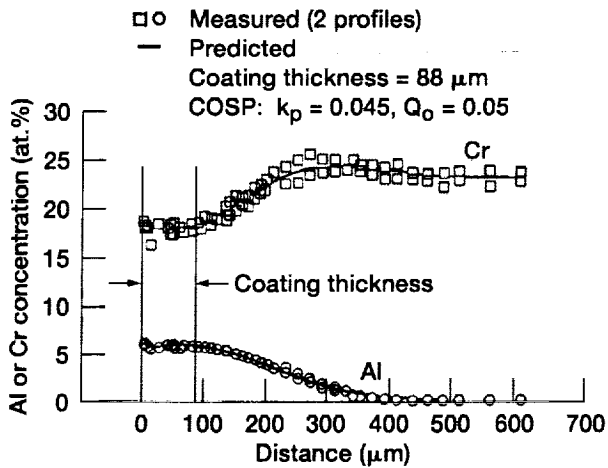


Figure 10.—A comparison of the actual and modelled (COSIM/COSP) diffusion profiles for a Ni-16Cr-25Al coating on a Ni-22Cr substrate (at.%) after cyclic oxidation at 1150 °C for 100 1-h cycles. (Nesbitt and Heckel, [19]).

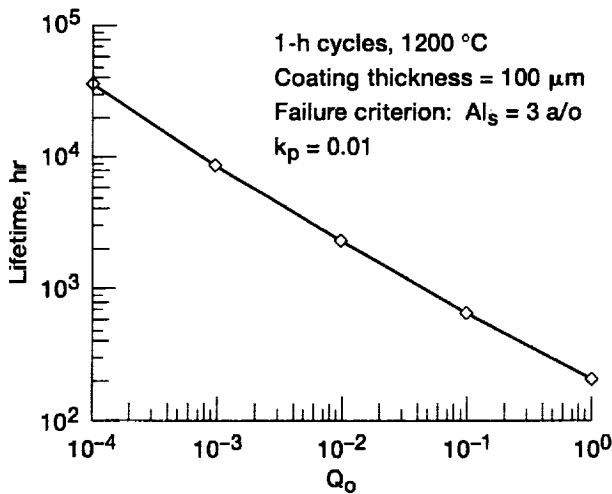


Figure 11.—Projected lifetimes for various spall constants  $Q_0$  (from COSIM/COSP models) for a Ni-20Cr-15Al coating on a Ni-10Cr-5Al substrate (at.%) after cyclic oxidation at 1200 °C using 1-h cycles. (Nesbitt, [22]).

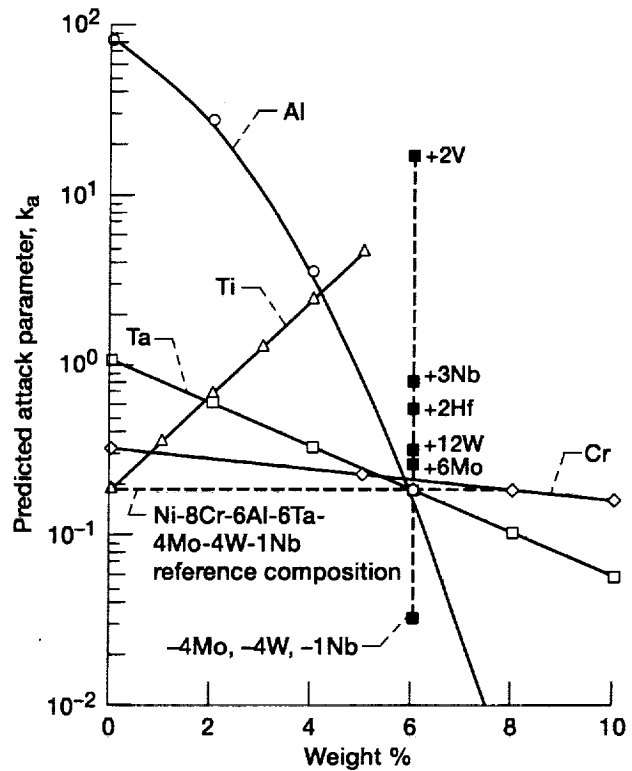


Figure 12.—The effect of individual elemental variations on the 1100 °C cyclic oxidation resistance attack parameter  $k_a$  for superalloys near the base composition of Ni-10Co-8Cr-6Al-6Ta-4W-4Mo-1Nb. ( $k_a$  is an empirically obtained figure of merit proportional to material recession as determined from a combination of the growth rate and final weight loss. The curves were calculated from a 15-term multilinear regression fit to oxidation data obtained on 34 commercial superalloys.) (Barrett, [26]; Smialek, Barrett, and Schaeffer, [28]).



REPORT DOCUMENTATION PAGE			Form Approved OMB No. 0704-0188	
Public reporting burden for this collection of information is estimated to average 1 hour per response, including the time for reviewing instructions, searching existing data sources, gathering and maintaining the data needed, and completing and reviewing the collection of information. Send comments regarding this burden estimate or any other aspect of this collection of information, including suggestions for reducing this burden, to Washington Headquarters Services, Directorate for Information Operations and Reports, 1215 Jefferson Davis Highway, Suite 1204, Arlington, VA 22202-4302, and to the Office of Management and Budget, Paperwork Reduction Project (0704-0188), Washington, DC 20503.				
1. AGENCY USE ONLY (Leave blank)	2. REPORT DATE February 2000	3. REPORT TYPE AND DATES COVERED Technical Memorandum		
4. TITLE AND SUBTITLE Cyclic Oxidation Testing and Modelling: A NASA Lewis Perspective			5. FUNDING NUMBERS WU-523-42-13-00	
6. AUTHOR(S) J.L. Smialek, J.A. Nesbitt, C.A. Barrett, and C.E. Lowell				
7. PERFORMING ORGANIZATION NAME(S) AND ADDRESS(ES) National Aeronautics and Space Administration John H. Glenn Research Center at Lewis Field Cleveland, Ohio 44135-3191			8. PERFORMING ORGANIZATION REPORT NUMBER E-12048	
9. SPONSORING/MONITORING AGENCY NAME(S) AND ADDRESS(ES) National Aeronautics and Space Administration Washington, DC 20546-0001			10. SPONSORING/MONITORING AGENCY REPORT NUMBER NASA TM-2000-209769	
11. SUPPLEMENTARY NOTES Prepared for the Cyclic Oxidation Workshop cosponsored by the Institute of Metals, European Federation of Corrosion, and DECHEMA, Frankfurt, Germany, February 25-26, 1999. Responsible person, James L. Smialek, organization code 5160, (216) 433-5500.				
12a. DISTRIBUTION/AVAILABILITY STATEMENT Unclassified - Unlimited Subject Category: 26 This publication is available from the NASA Center for AeroSpace Information, (301) 621-0390.			12b. DISTRIBUTION CODE Distribution: Nonstandard	
13. ABSTRACT (Maximum 200 words) The Materials Division of the NASA Lewis Research Center has been heavily involved in the cyclic oxidation of high temperature materials for 30 years. Cyclic furnace and burner rig apparatus have been developed, refined, and replicated to provide a large scale facility capable of evaluating many materials by a standard technique. Material behavior is characterized by weight change data obtained throughout the test, which has been modelled in a step-wise process of scale growth and spallation. This model and a coupled diffusion model have successfully described cyclic behavior for a number of systems and have provided insights regarding life prediction and variations in the spalling process. Performance ranking and mechanistic studies are discussed primarily for superalloys and coating alloys. Similar cyclic oxidation studies have been performed on steels, intermetallic compounds, thermal barrier coatings, ceramics, and ceramic composites. The most common oxidation test was performed in air at temperatures ranging from 800° to 1600 °C, for times up to 10,000 h, and for cycle durations of 0.1 to 1000 h. Less controlled, but important, test parameters are the cooling temperature and humidity level. Heating and cooling rates are not likely to affect scale spallation. Broad experience has usually allowed for considerable focus and simplification of these test parameters, while still revealing the principal aspects of material behavior and performance. Extensive testing has been performed to statistically model the compositional effects of experimental alloys and to construct a comprehensive database of complex commercial alloys.				
14. SUBJECT TERMS Alloys; Turbines; Oxidation			15. NUMBER OF PAGES 24	
			16. PRICE CODE A03	
17. SECURITY CLASSIFICATION OF REPORT Unclassified	18. SECURITY CLASSIFICATION OF THIS PAGE Unclassified	19. SECURITY CLASSIFICATION OF ABSTRACT Unclassified	20. LIMITATION OF ABSTRACT	